Cellulose (2019) 26:4391–4403
https://doi.org/10.1007/s10570-019-02377-1

ORIGINAL RESEARCH

Freeze dried cellulose nanocrystal reinforced unsaturated polyester composites: challenges and potential

Edward DiLoreto · Ejaz Haque · Arielle Berman · Robert J. Moon · Kyriaki Kalaitzidou

Received: 20 December 2018 / Accepted: 12 March 2019 / Published online: 16 March 2019

Abstract Functionalized cellulose particles were studied as a potential reinforcement for an unsaturated polyester resin (UPR) system, a common material for automotive applications of fiber reinforced plastics. A preliminary process for incorporating freeze-dried cellulose nanocrystal (CNC) powder into UPR was developed. Three surface chemistries were explored including sulfonated, methyl(triphenyl) phosphonium (PhCNC), and maleic acid (MCNC). By optical microscopy the filler was seen to be agglomerated within the matrix. Fractography showed that these agglomerates acted as stress concentration points resulting in decreased tensile and flexural strength. With the addition of 1 wt% CNCs, the flexural and tensile modulus increased by up to 53% and 22%, respectively. Dynamic mechanical analysis indicated that the PhCNC- and MCNC-UPR samples had a 61% and 66% higher glassy modulus than neat UPR, respectively. Despite the lack of nano-scale dispersion of CNC in UPR, these results reflect potential in the use of functionalized CNC agglomerates as an additive in UPR systems to produce composites with high moduli and good thermo-mechanical stability.

Keywords Unsaturated polyester · Cellulose nanocrystals · Functionalized nanoparticles

E. DiLoreto (✉) · E. Haque · R. J. Moon · K. Kalaitzidou
School of Materials Science and Engineering, Georgia Institute of Technology, Atlanta, USA
e-mail: etdiloreto@gatech.edu

A. Berman · K. Kalaitzidou
Georgia Tech Manufacturing Institute, G.W. Woodruff School of Mechanical Engineering, Atlanta, USA

R. J. Moon
The Forest Products Laboratory, U.S. Forest Service, Madison, USA

Introduction

Unsaturated polyester resin (UPR) is a prominent matrix material in automotive glass fiber reinforced plastic composites. UPRs are used due to their low cost and good mechanical properties (Biron 2018; Holbery and Houston 2006). In this application a reduction in density of the auto body can result in substantial benefits in terms of fuel efficiency and carbon footprint (Quadrennial Technology Review: An Assessment of Energy Technologies and Research Opportunities 2015). Therefore, improving mechanical properties per unit density is desired. The first step to achieving this is developing a scalable method for the addition of low-density reinforcement phase within the UPR to create a new resin formulation that can be utilized in automotive industry. Nanofillers such as montmorillonite, carbon nanotubes, and alumina have been studied in combination with UPR by direct addition for enhancing mechanical properties (Baran Inceoglu and Yilmazer 2003; Baskaran et al.

2011; Seyhan et al. 2007). Alumina nanoparticles have been shown to increase the tensile and flexural strength of UPR by 14 and 10% respectively at a filler content of 5 wt% (Baskaran et al. 2011). The addition of 5 wt% organically treated montmorillonite to UPR increased the tensile modulus by 16%, and tensile strength by 8%. (Baran Inceoglu and Yilmazer 2003). Amino functionalized double walled carbon nanotube—UPR composites showed a 15% increase in tensile strength at a loading of 0.5 wt% (Seyhan et al. 2007). The most commercially successful nanofillers are combined with polymer without the use of dispersing solvents (Fink 2017).

Toward this end, cellulose nanomaterials (CNMs) have been extensively studied for their potential as a versatile and functional biorenewable material. One type of CNM, cellulose nanocrystals (CNC), are spindle-shaped particles (3–20 nm in width and 50–500 nm in length), typically produced by sulfuric acid hydrolysis of wood pulp (Moon et al. 2011). CNCs have a unique combination of characteristics such as tensile strength of $\sim$ 3 GPa, stiffness of 110–220 GPa, high aspect ratio, low density, biodegradable, renewable, and low toxicity that make them an ideal nano-scale reinforcement for polymers as compared to other inorganic nanofillers (Elazzouzi-Hafraoui et al. 2008; Kumar et al. 2014; Lahiji et al. 2010; Moon et al. 2011; Roman 2015; Rusli and Eichhorn 2008). In particular their high aspect ratio can provide excellent load transfer from matrix to CNC. Previous work with silanized CNC showed a 20% improvement in tensile strength at 2 wt% loading, a competitive ehnacement with other, denser inorganic nanofillers (Baran Inceoglu and Yilmazer 2003; Baskaran et al. 2011; Kargarzadeh et al. 2015). The major challenge, as in the case of all nano-size reinforcements, is homogeneous nano-scale dispersion and uniform distribution of the CNCs within the polymer that can enable full realization of their reinforcing potential. And, furthermore, accomplishing this through industrially scalable means.

With their high stiffness and low density, CNC offers a potential enhancement in modulus of UPR without any weight penalty. This novel resin of CNC dispersed into UPR would then have the potential to decrease the amount of glass fiber needed to achieve the equivalent or higher mechanical properties to those of typical glass fiber/polyester composites commonly used (Mallick 2007). CNCs have previously been combined with a wide variety of thermoplastics, including poly lactic acid, polyvinyl acetate, polystyrene, and polyethylene (Garcia de Rodriguez 2006; Kamal and Khoshkava 2015; Lee et al. 2014; Lin and Dufresne 2013; Lin et al. 2011; Mariano et al. 2014; Sapkota et al. 2017). Less focus in the literature is placed upon thermoset-CNC composites due to the more complex processing challenges posed, such as dispersing nanomaterial in a viscous resin, a limited processing window, and elevated curing temperatures (Asadi et al. 2017; Muzzy and Kays 1984; Peng et al. 2017). An enhancement in impact and tensile properties of amino-silanized CNC reinforced UPR has been reported but it is noted that the CNC was dispersed in styrene and then excess styrene was evaporated (Kargarzadeh et al. 2015), a process that is not appealing to industry due to difficulties with process scale up.

Developing a scalable process for incorporation of CNCs into a thermoset such as thick UPR resin comes with a set of challenges. Perhaps most importantly, the material needs to be combined into a system with minimal use of dispersing solvents, (e.g., dimethylformamide, toluene, tetrahydrofuran, hexanes), which are highly regulated as they are environmentally problematic (Capello et al. 2007; Peng et al. 2017). CNCs are known to be strongly hydrophilic, which leads to agglomeration in organic systems, poor interfacial interactions, and ultimately a weaker composite system as compared to the pure matrix polymer (Kargarzadeh et al. 2015; Peng et al. 2017). To help mitigate this issue, the chemistry of the CNC surface can be altered so that it is more compatible with the matrix polymer. Tailoring the surface chemistry can enhance dispersibility in certain resin systems and, if reactive sites are added, it is possible to form chemical crosslinks between matrix and nanofiller (Lin et al. 2003). CNCs have been functionalized with vinyl, maleic, and a variety of silane groups (Brand et al. 2017; Habibi 2014; Selulosa-Polivinilklorida et al. 2015; Wang et al. 2017). Silanization is a prominent type of functionalization for nanofillers as the reaction is easily achievable on a benchtop scale. However, for larger industrial practices the rinsing process is unattractive due to the large volumes of waste produced. Other functionalization processes such as acid hydrolysis by functional acids, and ion exchange point towards a more reliable target for industrial applications. Acid hydrolysis is already the primary

industrial method for isolating CNCs from biomass precursors (Moon et al. 2011; Reid et al. 2017). Ion exchange processes are a proven technology and are commonly used in across a range of industries (Helfferich 1995).

To achieve a more commercially viable process for CNM incorporation into UPR a dry starting material is necessary. Dry CNM powders can be produced from a variety of methods (e.g., freeze-drying, spray-drying, etc.) (Abdallah and Kamal 2018; Khoshkava and Kamal 2014; Peng et al. 2013, 2012). During drying the CNMs agglomerate forming solid, hard, often non-porous particles that are tens to hundres of microns in size. The resulting particle size and morphology is highly dependent on the drying method/approach and parameters (Abdallah and Kamal 2018). As a result of the strong, inter-particle hydrogen bonds between CNM particles, one of the major challenges of dry CNM powders is maintaining the CNM nano-scale dimensions, not only in the dry state, but especially when re-dispersing them in solvents and polymer resins, and thus presenting a serious composite processing challenge and limiting the full potential of CNM powders to reinforce polymer materials (Khoshkava and Kamal 2014). One approach to alter the re-dispersion of CNM powders is to alter the surface chemistry of the starting CNMs prior to the drying process, by doing so it will alter the inter-particle bonding between CNM, in addition the new chemistry can make the CNM more compatible with a given polymer matrix materials, both of which should increase the possibilities of disintegrating CNM agglomerates. This is the approach considered in this study.

In this study, the effect of CNC surface treatment on the UPR composite mechanical properties, curing, and mechano-thermal behavior was examined. Unique to this study, was incorporation of CNC-functionalized materials to UPR without the use of dispersing solvent. To do this, CNC functionalized with three different chemistries, while in the dispersed state, were freeze-dried, and the resulting powders were directly mixed into a UPR matrix. The surface chemistries of the CNC studied were: polar sulfate ester as commonly found in industrial CNC production, nonpolar methyl(triphenyl) phosphonium produced by ion exchange, which reduces CNC–CNC interaction potential, and maleic acid ester, which has reactive unsaturated carbon–carbon bonds (Fox et al. 2016). Freeze drying was used in this study due to the small scale of the CNC material used, though not completely applicable to industry scaling up, the dispersibility of the resulting powders still provides some insight as what to expect from CNC powders produced from more industrial drying methods like spray drying. The UPR used was similar to that found in automotive sheet molding compound (SMC) fiber reinforced composites used in industry.

Materials

Freeze dried CNCs with different surface functionality and dimensions were used in this study. As received freeze-dried powder of sulfonated CNC (SCNC), manufactured by USDA-forest product laboratory (FPL) with a degree of substitution of 0.27 mmol/g, were purchased from the Process Development Center at the University of Maine. SCNC diameter and length post-hydrolysis were 7 ± 2 nm and 134 ± 52 nm respectively (Reid et al. 2017). Cellulose nanocrystals functionalized with Methyl(triphenyl) phosphonium (PhCNC), at a degree of substitution of 0.25 mmol/g, were provided courtesy of American University, Washington, D.C. at a concentration of 4 wt% in deionized (DI) water. PhCNC are produced from an ion exchange process. The average diameter and length of the PhCNC in solution were 6 ± 2 nm and 130 ± 67 nm respectively. Maleic acid functionalized CNC (MCNC) were provided courtesy of the Forestry Products Laboratory at a concentration of 0.58 wt% in DI water. MCNC were produced from bleached eucalyptus pulp fibers by maleic acid hydrolysis and have a diameter of 12–15 nm and a length of 500–700 nm, and a COOH degree of substitution of 0.20–0.25 mmol/g. Methods for synthesis and characterization of the PhCNC and MCNC materials can be found elsewhere (Fox et al. 2016; Wang et al. 2017). The as received MCNC and PhCNC water suspensions were freeze-dried by first mixing with 10% tert-Butyl alcohol by volume to enhance CNC isolation in the lyophilized state (Jiang and Hsieh 2014). The suspensions were then sonicated and placed in a $-$ 80 °C freezer. Once frozen samples were lyophilized until dry using a Labconco 12L freeze-drier at approximately $-$ 45 °C and 200 μbar for 2–4 days. Freeze-dried CNC powders, consisting of micronized particles/flakes, were used without any

post processing. Unsaturated polyester resin POLYLITE 31608-00 was provided courtesy of Reichhold, an industrial manufacturer of unsaturated polyester resins for composites and coatings. The initiator used, methyl ethyl ketone peroxide (MEKP), was purchased from Sigma-Aldrich. The catalyst, cobalt naphthenate (CoNap), was purchased from Alfa Aesar.

Experimental

Composite processing

Mixtures of freeze-dried CNC powders with UPR were produced first through manual stirring and then by probe sonication, QSonica Q-500 with ½″ probe, for 15 min, at 50% power alternating 5 s on and 3 s off, in an ice bath. Samples were cooled to room temperature at intervals of 2.5 min during sonication. Subsequently, the catalyst, CoNap was added to the mixture at 0.2 wt% and combined, followed by the initiator MEKP at 1.5 wt%. After mixing the system was degassed under vacuum, a small amount was set aside for optical imaging, while the remainder was poured into a silicone mold. The samples were cured at room temperature for 3.5 h and post cured at 100 °C for 30 min. A schematic representation of the composite processing path is shown in Fig. 1. MEKP was selected over other manufacturer recommended initiators because the higher temperatures required for other initiators could cause thermal degradation of the CNCs. Because of this alternative cure cycle the base properties of the neat UPR were expected to vary somewhat from manufacturer reported values as their curing agent and time/temperature profile were different. The concentration of CNCs within the composites was 1 wt% for each surface functionalization, this is a similar concertation level as what is done with other nanofillers in industry, and was used to in this study to explore the effect of surface modification on composite processing and mechanical properties. Additionally, for the PhCNC material, a higher concentration of 2 wt% CNC was also produced and tested to explore the effects of doubling the CNC concertation. Samples are referred to by *n*XCNC where *n* is the weight fraction, by total resin mixture, of CNC and *X* refers to the functionalization or type of CNC used. Baseline unfilled UPR samples are referred to simply as UPR or neat UPR.

Material characterization

Optical imaging of CNC-UPR mixtures was completed using a Leica DM2500 optical microscope to observe nanomaterial dispersion quality. The small amount of resin mixture that was set aside just after the

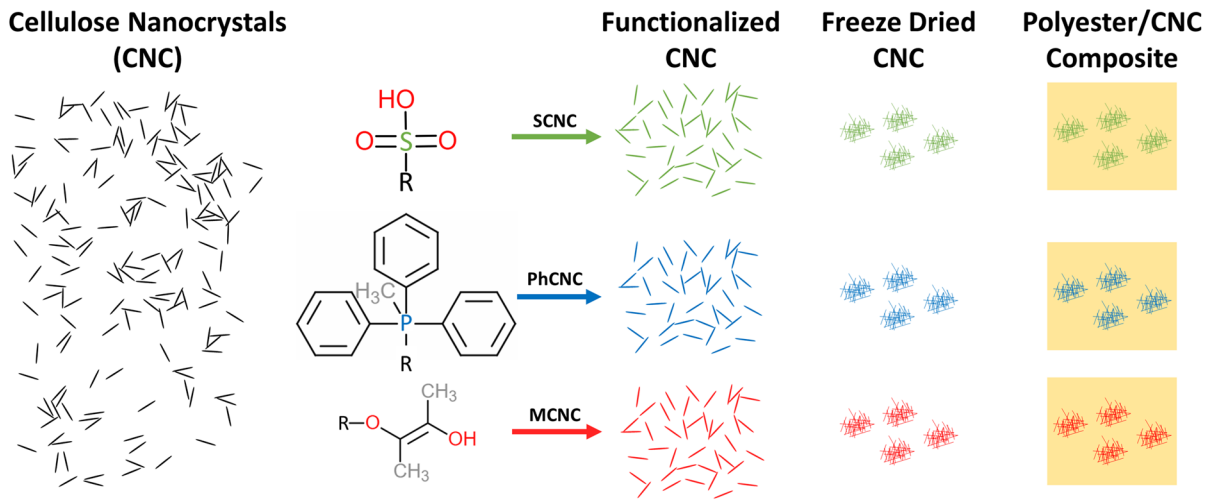

Fig. 1 Schematic showing the process for incorporation of CNC into polyester composite. Cellulose nanocrystals (CNCs) are dispersed and the surface of individual CNCs were functionalized with either polar sulfate ester (green), nonpolar methyl(triphenyl) phosphonium (blue), and maleic acid ester (red). The functionalized CNCs are freeze dried, which creates agglomerated CNC particles ~ 100 µm in size. Finally, freeze-dried CNC powers are mixed within UPR, and the agglomerated CNC particles are retained within the composite. (Color figure online)

degassing step was poured onto a glass microscope slide and covered with a glass cover slip, such that the layer of CNC-UPR mixture was about 180 μm thick. Images were collected under transmission.

Mechanical testing of the tensile strength and modulus were completed according to ASTM D638 using an Instron 5982 equipped with a 100 kN load cell. A preload of 20 N was applied to remove slack from the load string, and testing was completed using displacement control with a cross-head speed of 5 mm/min (Committee 2014). Testing was completed in ambient conditions. The dogbone neck sample thickness and width were 3.3 mm, and an extensometer MTS-Model-634, with a gauge length of 12.7 mm and an axial travel range of ± 10% was used to record the axial strain. Six specimens for each CNC-UPR composite type were tested. The tensile modulus was calculated in the linear elastic region, (1.1–1.25% strain).

Mechanical testing of the flexural strength and modulus were completed according to ASTM D790-17 using an Instron 33R 4466 equipped with a 500 N load cell (Committee 2017). Sample dimensions were 60 mm × 11.9 mm × 3.6 mm, and were tested in 3-pt bending with a span length of 50 mm, and a displacement rate of 1.18 mm/min. Testing was completed in ambient conditions. At least four specimens of each CNC-UPR composite type were tested. Flexural modulus was taken as the linear regression in the linear elastic region, (1.0–1.1% strain).

Dynamic mechanical analysis (DMA) was used to determine the glass transition temperature (T_g) following ASTM D7028-07 (Committee 2015). The DMA parameters were standard at an oscillation of 1 Hz and a heating rate of 3 °C/min, ramped from 40 to 230 °C. Sample dimensions were 60 mm × 11.9 mm × 3.6 mm, and were tested in 3-pt bending with a span length of 43.3 mm and a strain of 0.1%. The T_g was defined as the temperature at peak tan(δ). Glassy and rubbery modulus were taken to be the storage modulus at 80 °C and 180 °C respectively. At least two specimens of each CNC-UPR composite type were tested.

Differential scanning calorimetry (DSC) was conducted using a TA Instruments Q2000 DSC on test specimens of approximately 10 mg. Samples were tested in Tzero Aluminum DSC pans and lids. To determine the residual enthalpy, two samples of each different curing cycle were ramped at 10 °C/min to 200 °C under a nitrogen purge of 50 mL/min. In addition to composite formulations, neat UPR resin was also tested under the same parameters to acquire the total enthalpy of cure, which was used to calculate the percent cure of each sample.

Electron microscopy was completed using a Zeiss Ultra 60 FESEM at an accelerating voltage of 5 kV. Prior to imaging, samples were gold sputter coated for 20 s using a Cressington 108 to reduce charging effects.

Density measurements were completed using the water displacement technique of specimens that weighed at least 300 mg. At least 3 specimens of each CNC-UPR composite type were tested.

All data herein is represented by a mean with one standard deviation as error bars.

Results

Morphology of freeze dried CNC

The surface functionalized CNC suspensions were freeze-dried prior to combining with the resin. Freeze-dried CNC powders were examined via field-emission scanning electron microscopy (FESEM), characteristic images of the freeze-dried powders can be seen in Fig. 2. SCNC, (Fig. 2a, d, g), was comprised of ∼ 200 μm particles with little visible porosity. Freeze-drying PhCNC produced ∼ 1 mm platelets with some visible surface porosity, Fig. 2b, e, h. Finally, MCNC, which was lyophilized from a lower solids content suspension, showed porosity with some fibrillation visible at high magnification, Fig. 2c, f, i. These differences in dry morphology could lead to different dispersion quality or structure within the resulting polymer composite. Notably, none of the freeze-dried CNC powders were in a nano-disperse state prior to combining with the resin. The freeze-dried CNC powders were mixed with the resin without any further preprocessing.

Distribution of freeze dried CNC in resin

Optical micrographs of the CNC-UPR mixtures are shown in Fig. 3. Optical imaging was done to observe the dispersion quality of the CNC in the UPR matrix. It is evident that a 100% nano-scale dispersion of the CNCs was not achieved, as all samples had

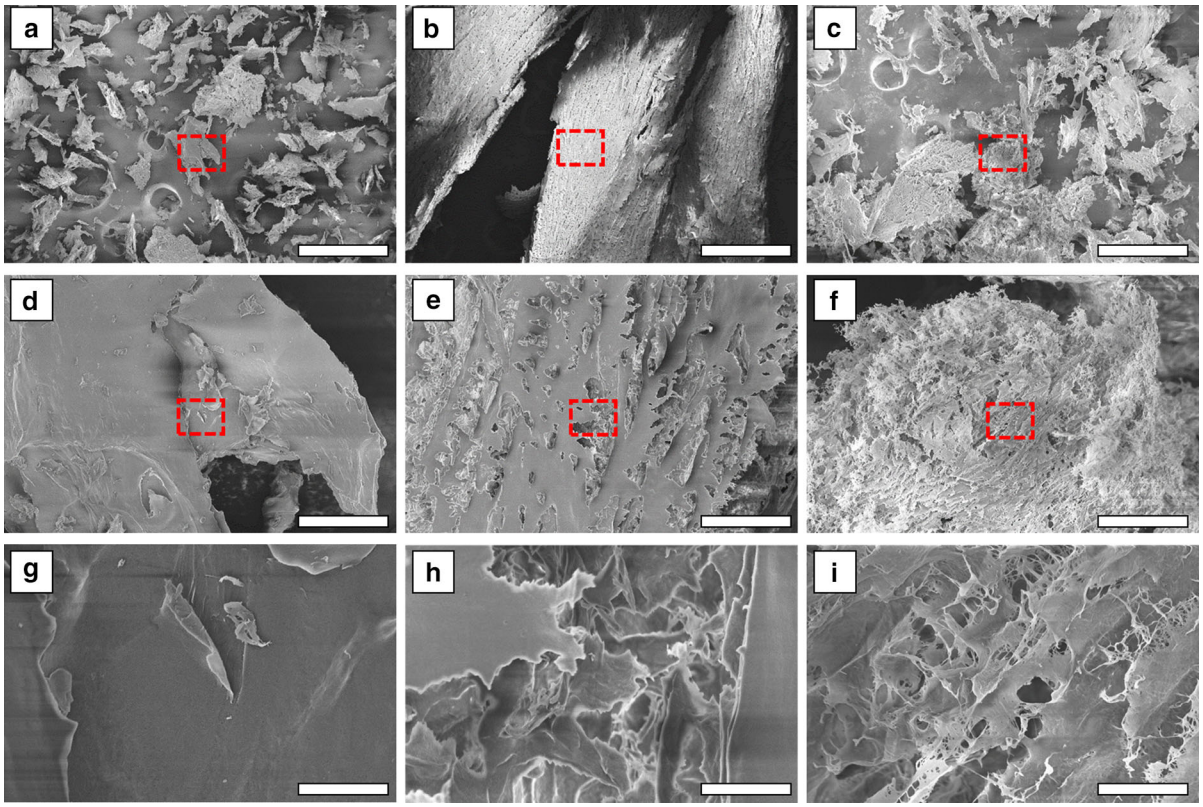

Fig. 2 FESEM micrographs of freeze-dried CNC,: **a**, **d**, **g** SCNC, **b**, **e**, **h** PhCNC, **c**, **f**, **i** MCNC. The dotted red box indicates the approximate location of the corresponding next higher magnification image of the sample. Scale bars are 500 μm for (**a–c**), 50 μm for (**d–f**), and 5 μm for (**g–i**)

agglomerates up to 100 μm (i.e., dark spots and flakes in images). This CNC agglomeration is primarily a result of the inability to break up and subsequently disperse the CNC freeze-dried flakes, which are of a similar size scale. The three different CNC surface functionalizations did not have much of an effect on this, which is interesting since the functionalization occurred before freeze-drying and should have some influence on the eutectic structure formed during freezing and thus the resulting scaffold formed after drying (De France et al. 2017; Han et al. 2013). Considering the micron-scale dispersion, the CNC agglomerates appear to be uniformly dispersed throughout the sample, and there is little influence from the different surface treatments. Because of this, the nano-scale dispersion of the CNC was not characterized, as the high degree of CNC agglomerated will dictate any mechanism responsible for changes in the mechanical properties (e.g., flaw size, critical length).

General material properties

The material properties for neat UPR and CNC-UPR composites are presented in Table 1. The CNC additions had minimal impact on the curing behavior and density. All composite samples had a satisfactory percent cure of greater than 90%, and a density of 1.23–1.24 g/mL, matching predictions from rule of mixtures. The glass transitions of specimens were observed through the position of the tan(δ) peak in DMA measurements. With respect to the UPR sample all CNC-UPR samples were within 1 standard deviation. As a result, it is difficult to conclude on the relative effect of CNC addition and CNC surface functionalization on the UPR properties. However, within CNC-UPR samples, the glass transition of 1MCNC composites was 11.5 °C higher than that of 1SCNC. It is hypothesized that the shift in the 1MCNC case may be due to a restriction of the polymer chains at the CNC interface through chemical crosslinks at

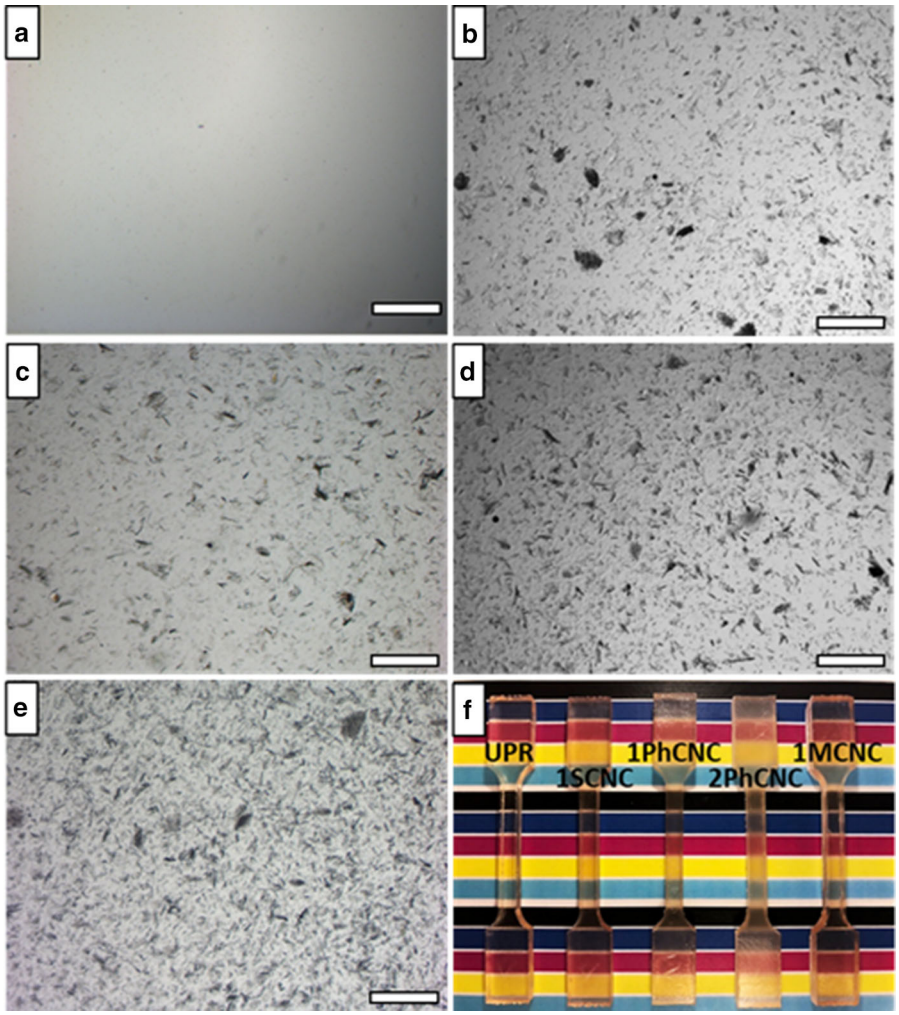

Fig. 3 Transmitted light micrographs of CNC-UPR mixtures (uncured) for: **a** UPR without filler, **b** 1SCNC, **c** 1MCNC, **d** 1PhCNC, **e** 2PhCNC, showing the extent of CNC agglomeration, and their flake-like morphology. Scale bars 500 µm. **f** Photograph of dogbone tensile testing specimens for neat UPR, 1SCNC, 1PhCNCC, 2PhCNC, and 1MCNC, respectively, showing differences in translucency between samples

Table 1 Properties of CNC-UPR composites, including degree of cure, T_g, and density

Composite	Degree of cure (%)	T_g (°C)	Density (g/mL)
UPR	99.5 ± 0.1	156.3 ± 9.0	1.23 ± 0.005
1SCNC	99.2 ± 0.3	148.5 ± 0.7	1.23 ± 0.003
1PhCNC	99.5 ± 0.1	152.5 ± 3.5	1.24 ± 0.002
2PhNC	98.5 ± 0.3	140.0 ± 10.4	1.24 ± 0.001
1MCNC	99.2 ± 0.1	160.0 ± 1.0	1.24 ± 0.002

the maleic group functional site (Khare et al. 2014; Ma et al. 2007).

Composite mechanical properties

Mechanical properties, tensile and flexural, are shown in Fig. 4. Mechanical testing is useful to benchmark

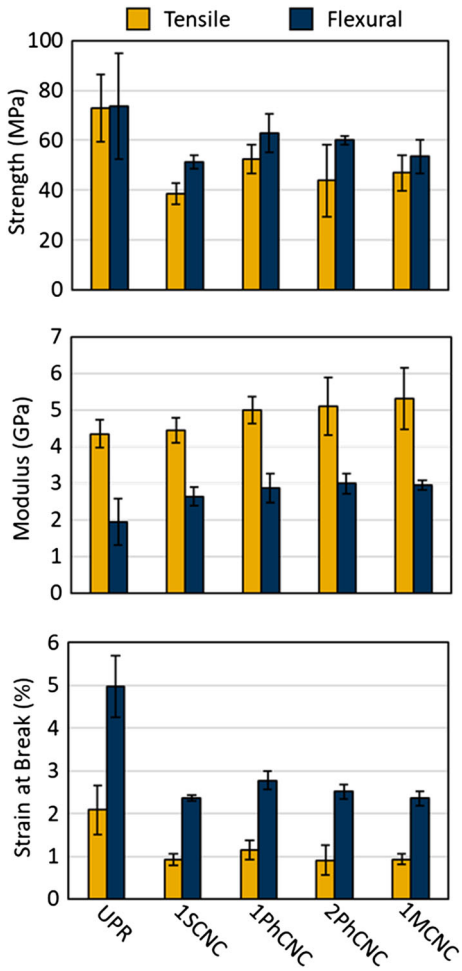

Fig. 4 Tensile and flexural properties of neat UPR, and CNC-UPR composites for the three types functionalized CNC. Addition of CNC increased the average tensile and flexural modulus but decreased the average tensile and flexural strength

the materials and acts as an indicator for material performance in applications such as glass fiber reinforced plastic matrices in auto bodies. In general, the CNC additions were shown to increase the tensile and flexural modulus and decrease both the tensile and flexural strength and strain to failure. Tensile results show an increase in tensile modulus for 1PhCNC, 2PhCNC, and 1MCNC samples over the 1SCNC and UPR samples. A maximum increase of 22% in tensile modulus was observed for 1MCNC over the UPR baseline. Likewise, flexural modulus increased with CNC additions, with a maximum increase of 53% for 2PhCNC. The effect of CNC surface chemistry can be assessed by considering that tensile modulus in short fiber reinforced materials is governed primarily by the critical length, and the aspect ratio, modulus, and volume fraction of the filler. Critical length is in turn determined by the interfacial interactions between the filler and matrix. Based on this data the effect of MCNC-UPR interactions does not result in a significantly different effect as compared to the filler-matrix interactions for PhCNC and SCNC, which have similar CNC aggregate size by optical microscopy. All the CNC-UPR composites had lower tensile and flexural strength as compared to UPR, which is believed to be caused from stress concentration sites arising from CNC agglomeration (see fractography section). Based on the data an increase of loading from 1 to 2 wt% PhCNC does not seem to have a significant effect on the flexural or tensile modulus or strength. Despite the micronized agglomeration of CNC, their addition to UPR appear to be a promising reinforcement for increasing the modulus of the matrix in glass fiber reinforced plastics.

Previous work on CNC-UPR composites by Kargarzadeh et al. (Kargarzadeh et al. 2015) produce a fine nano-size scale dispersion of the CNCs within the UPR by using an approach where freeze-dried silane treated CNCs were pre-dispersed in styrene prior to composite processing. They reported a 20% increase in tensile strength and 10% in tensile modulus at 2 wt% CNC as compared to the neat UPR. The key to the increase in tensile strength with CNC additions was the ability to form a fine CNC dispersion within the UPR. In contrast, in the current study, a fine nano-size scale CNC dispersion was not obtained and the agglomerated CNCs acted as stress concentration points that hastened failure and resulted in lower tensile strengths of the CNC-UPR composites. Interestingly, both studies show increases in tensile modulus despite the contrasting levels of CNC dispersion of within UPR, suggesting the state of CNC dispersion within the UPR has less of an impact as opposed to other factors, such as, differences in interfacial interactions. Lastly, it should be noted that the pre-dispersion of CNC in styrene approach used by Kargarzadeh et al., was not used in the current study, as using large volumes of styrene to pre-disperse the cellulose is environmentally and occupationally hazardous and contradictory to the objective of industrially applicable process development.

Crack initiation sites

To assess possible mechanisms for the reduced tensile and flexural strength of UPR from the CNC additions the fracture surfaces of the tensile samples (Fig. 5) were examined. For the UPR, a flat and smooth fracture planes perpendicular to the direction of loading were observed and is indicative of a brittle fracture behavior of polymer materials and is expected for the type of UPR used in this study. The UPR

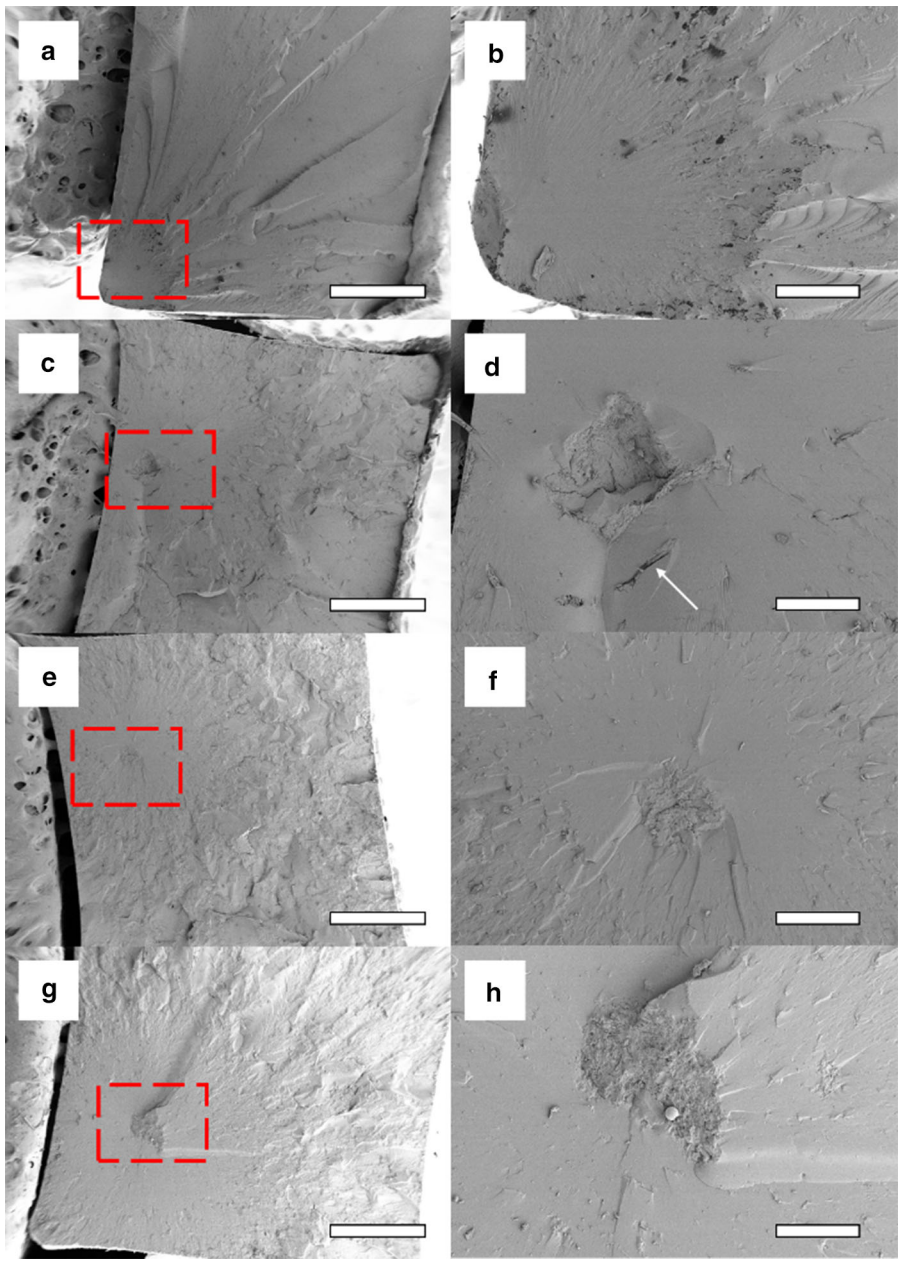

Fig. 5 FESEM micrographs of tensile fracture surfaces for: **a**, **b** neat UPR, **c**, **d** 1SCNC, **e**, **f** 1PhCNC, and **g**, **h** 1MCNC. The lower magnification images (**a**, **c**, **e**, **g**) show entire fracture surface, scale bars 1 mm, while higher magnification images (**b**, **d**, **f**, **h**) show the corresponding crack initiation sights, scale bars 200 µm. The dotted red box shows the location of the crack initiation point, and the location of the corresponding higher magnification images. White arrow in **d** indicates delamination at CNC agglomeration-UPR interface. (Color figure online)

samples show crack initiation sites located at the edge of the test specimen (Fig. 5 a), which indicates a homogenous material with a defect size smaller than what is at the surface of the test specimen. In contrast, for all CNC-UPR composites, crack initiation occurred within the bulk of the test specimen at a localized stress concentration point (Fig. 5 f, g, h). These crack initiation sites are of a similar size-scale to that of the CNC aggregates, (Fig. 3), indicating that the CNC aggregates are causing property limiting defects within the composites. However, the fracture surface away from the initiation point (Fig. 5 b, c, d), appeared to be more textured as compared to the UPR, indicating more resistance to crack propagation. This suggest that if the larger defects can be removed, and thus remove the crack initiation points, it may be possible to increase the strength of UPR by CNC additions. The effect of CNC surface chemistry was not overwhelmingly apparent, however, for SCNC-UPR it was easier to see the flake shaped CNC aggregates and interfacial delamination to the UPR (Figs. 5 d, 6), which were not as apparent for the PhCNC and MCNC composites. This may suggest stronger bonding between PhCNC and MCNC to the UPR as compared to the SCNC.

Composite thermomechanical properties

To help assess the interaction between CNC agglomerates and the UPR matrix, and the effect of CNC surface chemistry, DMA analysis was conducted. This technique provides an approach to probe the filler-matrix interface and interphase region within the system. For the CNC-UPR system, the interphase region extends from the CNC-UPR interface to some depth within the UPR, this region would be expected to have different physical properties than the bulk UPR. The properties and size of this interphase are expected to depend on the surface chemistry of the CNC. It is generally expected that polymer chains located in this interphase have a more restricted range of motion resulting in more elastic behavior as compared to the bulk. Furthermore, the temperature dependence of interphase properties, which can provide further insight to the matrix-filler interaction are probed by DMA. A weaker interaction would result in a smaller interphase by volume and a lower storage modulus, while strong interactions can produce an increase in storage modulus, and higher thermo-mechanical stability (i.e. less change in modulus with temperature). For example, a fully cross-linked and nanodisperse filler would be expected to have a high storage modulus and a smaller reduction in storage modulus above the T_g. By assessing shifts in storage modulus associated with CNC additions, the effect of the CNC surface chemistry can be observed.

DMA measurements at 80 °C, assessed the glassy storage modulus, in which the 1MCNC and 1PhCNC showed a 61% and 66% improvement, respectively, in glassy storage modulus over the neat UPR sample (Fig. 7). Notably, the 1MCNC and 1PhCNC are also shown to have higher glassy storage modulus as compared to 1SCNC. The similar magnitude of the

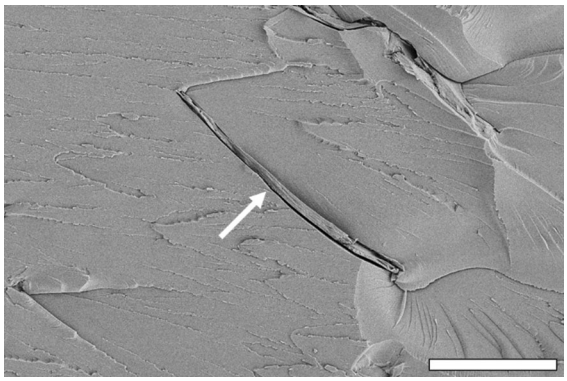

Fig. 6 FESEM micrograph of tensile fracture surface for 1SCNC, showing CNC agglomerate flake (indicated by the arrow) and delamination along the interface with the UPR matrix. Scale bar 500 μm

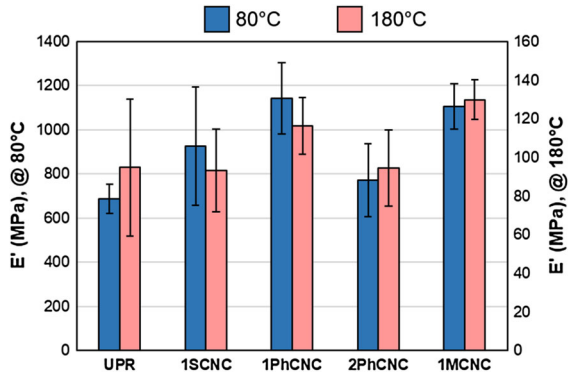

Fig. 7 Storage moduli of CNC-UPR composites in the glassy (at 80 °C) and rubbery states (at 180 °C). Addition of CNC enhanced the average glassy modulus across all formulations. PhCNC and MCNC increased the average rubbery modulus at 1 wt% loading

1MCNC and 1PhCNC glassy modulus indicate that the surface chemistries likely have similar effects on the system structure. With respect to 1MCNC it is possible that a more elastic interphase is the result of chemical crosslinking of the polymer matrix through the maleic group on the CNC surface (Benoit et al. 2000; Suo et al. 2007). As shown previously, the phenyl groups in PhCNCs sterically hinder CNC–CNC interactions (Fox et al. 2016). It is conceivable that a reduction in CNC–CNC interaction energy potential would lead to relatively more CNC-matrix interactions. This phenomenon could result in a larger interphase volume relative to an SCNC case and as a result a higher storage modulus. Note that the CNC agglomeration in this study reduces the effective volume of the interphase region, and is expected to result in a smaller effect on the storage modulus, as compared to a fully nano-scale CNC dispersed within the UPR system.

Interestingly, the glassy modulus of the 2PhCNC is 32% lower than that of 1PhCNC, while the tensile and flexural moduli are consistent between the two samples. The difference in length scales of the techniques may be the source of an explanation. DMA probes the filler-matrix interface within the system, while tensile and flexural testing examine the bulk. Furthermore, the temperature at which the glassy modulus is given, 80 °C, is elevated to the flexural and tensile testing, which were conducted in ambient conditions. Taken overall, the data would indicate that the agglomeration of CNC in the 2PhCNC case is significant enough to affect the nanoscale interactions, as observed through DMA, but not enough to change the bulk behavior, as observed through macromechanical techniques.

DMA measurements at 180 °C, assessed the rubbery storage modulus, and revealed somewhat similar results, in which the 1MCNC and 1PhCNC showed the greatest increase in storage modulus, 65% and 48%, respectively, over the UPR baseline. Here MCNC appears to provide a moderately more effective reinforcement as compared to the PhCNC. The MCNC-UPR interactions are to some extent more thermally stable than the PhCNC-UPR interactions.

Conclusion

The effect of surface functionalized of cellulose nanocrystals: sulfate ester (SCNC), methyl(triphenyl) phosphonium (PhCNC), and maleic acid ester (MCNC), on freeze-drying CNC agglomerate morphology, and the resulting properties of unsaturated polyester (UPR)-CNC composites was studied. The addition of freeze dried CNC powders into UPR, resulting in micron-sized CNC agglomerates, were shown to enhance the flexural and tensile modulus by up to 53% and 22%, respectively, but decreased the tensile strength. The 1PhCNC-UPR and 1MCNC-UPR composites, showed a 66% and 61% increase in glassy modulus and a 65% and 48% increase in rubbery modulus over the UPR baseline, respectively. Additionally, the glass transition increased by 4.5 °C and 12 °C for 1PhCNC and 1MCNC over 1SCNC, respectively.

While ideal nano-scale dispersions of CNC in UPR were not achieved, the results in this work reflect potential in the use of functionalized CNC agglomerates as an additive in SMC systems to produce composites with high moduli and good thermo-mechanical stability without dramatically affecting overall cure performance. They also serve to outline a processing pathway for CNC-UPR composites while identifying key challenges along said pathway that must be addressed in any work involving the use of CNC as a nanofiller, such as the redispersion of freeze-dried CNCs in UPR resins.

Acknowledgments This work was supported by P^3 Nano and the U.S. Endowment for Forestry and Communities. The authors would like to thank Prof. Douglas M. Fox from the American University and Prof. J.Y. Zhu from Forest Products Laboratory for providing the functionalized CNC studied in this work, as well as Reichhold for providing the polyester resin. The authors would also like to thank their colleagues at Georgia Tech, namely Prof. Jon Colton for providing mechanical testing equipment, Prof. Satish Kumar for providing the optical microscope, the staff of the Materials Characterization Facility, and Mr Nicholas Billeter and Mr Joshua Oswald for assisting with tensile and flexural measurements.

References

Abdallah W, Kamal MR (2018) Influence of process variables on physical characteristics of spray freeze dried cellulose nanocrystals. Cellulose 25:5711–5730. https://doi.org/10.1007/s10570-018-1975-0

Asadi A, Miller M, Singh AV, Moon RJ, Kalaitzidou K (2017) Lightweight sheet molding compound (SMC) composites containing cellulose nanocrystals. Compos Struct 160:211–219. https://doi.org/10.1016/j.compstruct.2016.10.051

Baran Inceoglu A, Yilmazer U (2003) Synthesis and mechanical properties of unsaturated polyester based nanocomposites. Polym Eng Sci 43:661–669. https://doi.org/10.1002/pen.10054

Baskaran R, Sarojadevi M, Vijayakumar CT (2011) Unsaturated polyester nanocomposites filled with nano alumina. J Mater Sci 46:4864–4871. https://doi.org/10.1007/s10853-011-5398-7

Benoit D, Hawker CJ, Huang EE, Lin ZQ, Russell TP (2000) One-step formation of functionalized block copolymers. Macromolecules 33:1505–1507. https://doi.org/10.1021/ma991721p

Biron M (2018) The Plastics Industry. In: Biron M (ed) Thermoplastics and thermoplastic composites. William Andrew Publishing, Norwich, pp 31–132. https://doi.org/10.1016/b978-0-08-102501-7.00002-3

Brand J, Pecastaings G, Sebe G (2017) A versatile method for the surface tailoring of cellulose nanocrystal building blocks by acylation with functional vinyl esters. Carbohydr Polym 169:189–197. https://doi.org/10.1016/j.carbpol.2017.03.077

Capello C, Fischer U, Hungerbuhler K (2007) What is a green solvent? A comprehensive framework for the environmental assessment of solvents. Green Chem 9:927–934. https://doi.org/10.1039/b617536h

Committee D (2014) Test method for tensile properties of plastics. ASTM International, West Conshohocken. https://doi.org/10.1520/D0638-14

Committee D (2015) Standard test method for glass transition temperature (DMA Tg) of polymer matrix composites by dynamic mechanical analysis (DMA). ASTM International, West Conshohocken. https://doi.org/10.1520/D7028-07E01R15

Committee D (2017) Standard test methods for flexural properties of unreinforced and reinforced plastics and electrical insulating materials. ASTM International, West Conshohocken. https://doi.org/10.1520/D0790-17

De France KJ, Hoare T, Cranston ED (2017) Review of hydrogels and aerogels containing nanocellulose. Chem Mater 29:4609–4631

Elazzouzi-Hafraoui S, Nishiyama Y, Putaux JL, Heux L, Dubreuil F, Rochas C (2008) The shape and size distribution of crystalline nanoparticles prepared by acid hydrolysis of native cellulose. Biomacromolecules 9:57–65. https://doi.org/10.1021/bm700769p

Fink JK (2017) Reactive polymers: fundamentals and applications: a concise guide to industrial polymers. William Andrew Publishing, Norwich

Fox DM et al (2016) Simultaneously tailoring surface energies and thermal stabilities of cellulose nanocrystals using ion exchange: effects on polymer composite properties for transportation, infrastructure, and renewable energy applications. ACS Appl Mater Interfaces 8:27270–27281. https://doi.org/10.1021/acsami.6b06083

Garcia de Rodriguez NL, Thielemans W, Dufresne A (2006) Sisal cellulose whiskers reinforced polyvinyl acetate nanocomposites. Cellulose 13:261–270. https://doi.org/10.1007/s10570-005-9039-7

Habibi Y (2014) Key advances in the chemical modification of nanocelluloses. Chem Soc Rev 43:1519–1542. https://doi.org/10.1039/c3cs60204d

Han J, Zhou C, Wu Y, Liu F, Wu Q (2013) Self-assembling behavior of cellulose nanoparticles during freeze-drying: effect of suspension concentration, particle size, crystal structure, and surface charge. Biomacromolecules 14:1529–1540. https://doi.org/10.1021/bm4001734

Helfferich FG (1995) Ion exchange. Courier Corporation, Chelmsford

Holbery J, Houston D (2006) Natural-fiber-reinforced polymer composites applications in automotive. Jom 58:80–86. https://doi.org/10.1007/s11837-006-0234-2

Jiang F, Hsieh YL (2014) Assembling and redispersibility of rice straw nanocellulose: effect of tert-butanol. ACS Appl Mater Interfaces 6:20075–20084. https://doi.org/10.1021/am505626a

Kamal MR, Khoshkava V (2015) Effect of cellulose nanocrystals (CNC) on rheological and mechanical properties and crystallization behavior of PLA/CNC nanocomposites. Carbohydr Polym 123:105–114. https://doi.org/10.1016/j.carbpol.2015.01.012

Kargarzadeh H, Sheltami RM, Ahmad I, Abdullah I, Dufresne A (2015) Cellulose nanocrystal: a promising toughening agent for unsaturated polyester nanocomposite. Polymer 56:346–357. https://doi.org/10.1016/j.polymer.2014.11.054

Khare KS, Khabaz F, Khare R (2014) Effect of carbon nanotube functionalization on mechanical and thermal properties of cross-linked epoxy-carbon nanotube nanocomposites: role of strengthening the interfacial interactions. ACS Appl Mater Interfaces 6:6098–6110. https://doi.org/10.1021/am405317x

Khoshkava V, Kamal MR (2014) Effect of cellulose nanocrystals (CNC) particle morphology on dispersion and rheological and mechanical properties of polypropylene/CNC nanocomposites. ACS Appl Mater Interfaces 6:8146–8157. https://doi.org/10.1021/am500577e

Kumar A, Negi YS, Choudhary V, Bhardwaj NK (2014) Characterization of cellulose nanocrystals produced by acid-hydrolysis from sugarcane bagasse as agro-waste. J Mater Phys Chem 2:1–8

Lahiji RR, Xu X, Reifenberger R, Raman A, Rudie A, Moon RJ (2010) Atomic force microscopy characterization of cellulose nanocrystals. Langmuir 26:4480–4488. https://doi.org/10.1021/la903111j

Lee KY, Aitomaki Y, Berglund LA, Oksman K, Bismarck A (2014) On the use of nanocellulose as reinforcement in polymer matrix composites. Compos Sci Technol 105:15–27. https://doi.org/10.1016/j.compscitech.2014.08.032

Lin N, Dufresne A (2013) Physical and/or chemical compatibilization of extruded cellulose nanocrystal reinforced polystyrene nanocomposites. Macromolecules 46:5570–5583. https://doi.org/10.1021/ma4010154

Lin Y, Zhou B, Fernando KAS, Liu P, Allard LF, Sun YP (2003) Polymeric carbon nanocomposites from carbon nanotubes functionalized with matrix polymer. Macromolecules 36:7199–7204. https://doi.org/10.1021/ma0348876

Lin N, Huang J, Chang PR, Feng JW, Yu JH (2011) Surface acetylation of cellulose nanocrystal and its reinforcing function in poly(lactic acid). Carbohydr Polym 83:1834–1842. https://doi.org/10.1016/j.carbpol.2010.10.047

Ma PC, Kim JK, Tang BZ (2007) Effects of silane functionalization on the properties of carbon nanotube/epoxy nanocomposites. Compos Sci Technol 67:2965–2972. https://doi.org/10.1016/j.compscitech.2007.05.006

Mallick P (2007) Fiber-reinforced composites. Dekker mechanical engineering. CRC Press, Boca Raton. https://doi.org/10.1201/9781420005981

Mariano M, El Kissi N, Dufresne A (2014) Cellulose nanocrystals and related nanocomposites: review of some properties and challenges. J Polym Sci Part B-Polym Phys 52:791–806. https://doi.org/10.1002/polb.23490

Moon RJ, Martini A, Nairn J, Simonsen J, Youngblood J (2011) Cellulose nanomaterials review: structure, properties and nanocomposites. Chem Soc Rev 40:3941–3994. https://doi.org/10.1039/c0cs00108b

Muzzy JD, Kays AO (1984) Thermoplastic vs thermosetting structural composites. Polym Compos 5:169–172. https://doi.org/10.1002/pc.750050302

Peng YC, Gardner DJ, Han YS (2012) Drying cellulose nanofibrils: in search of a suitable method. Cellulose 19:91–102. https://doi.org/10.1007/s10570-011-9630-z

Peng YC, Gardner DJ, Han Y, Kiziltas A, Cai ZY, Tshabalala MA (2013) Influence of drying method on the material properties of nanocellulose I: thermostability and crystallinity. Cellulose 20:2379–2392. https://doi.org/10.1007/s10570-013-0019-z

Peng SX, Shrestha S, Yoo Y, Youngblood JP (2017) Enhanced dispersion and properties of a two-component epoxy nanocomposite using surface modified cellulose nanocrystals. Polymer 112:359–368. https://doi.org/10.1016/j.polymer.2017.02.016

Quadrennial technology review: an assessment of energy technologies and research opportunities (2015)

Reid MS, Villalobos M, Cranston ED (2017) Benchmarking cellulose nanocrystals: from the laboratory to industrial production. Langmuir 33:1583–1598. https://doi.org/10.1021/acs.langmuir.6b03765

Roman M (2015) Toxicity of cellulose nanocrystals: a review. Ind Biotechnol 11:25–33. https://doi.org/10.1089/ind.2014.0024

Rusli R, Eichhorn SJ (2008) Determination of the stiffness of cellulose nanowhiskers and the fiber-matrix interface in a nanocomposite using Raman spectroscopy. Appl Phys Lett 93:033111. https://doi.org/10.1063/1.2963491

Sapkota J, Natterodt JC, Shirole A, Foster EJ, Weder C (2017) Fabrication and properties of polyethylene/cellulose nanocrystal composites. Macromol Mater Eng 302:1600300. https://doi.org/10.1002/mame.201600300

Selulosa-Polivinilklorida SRN, Sheltami RM, Kargarzadeh H, Abdullah I (2015) Effects of silane surface treatment of cellulose nanocrystals on the tensile properties of cellulose-polyvinyl chloride nanocomposite. Sains Malays 44:801–810

Seyhan AT, Gojny FH, Tanoğlu M, Schulte K (2007) Critical aspects related to processing of carbon nanotube/unsaturated thermoset polyester nanocomposites. Eur Polym J 43:374–379. https://doi.org/10.1016/j.eurpolymj.2006.11.018

Suo AL, Qian JM, Yao Y, Zhang WG (2007) Synthesis and properties of carboxymethyl cellulose-graft-poly(acrylic acid-co-acrylamide) as a novel cellulose-based superabsorbent. J Appl Polym Sci 103:1382–1388. https://doi.org/10.1002/app.23948

Wang RB, Chen LH, Zhu JY, Yang RD (2017) Tailored and integrated production of carboxylated cellulose nanocrystals (CNC) with nanofibrils (CNF) through maleic acid hydrolysis. Chemnanomat 3:328–335. https://doi.org/10.1002/cnma.201700015